Atmospheric Research 172–173 (2016) 109–118

Contents lists available at ScienceDirect

Atmospheric Research

journal homepage: www.elsevier.com/locate/atmosres

Application of the Doppler weather radar in real-time quality control of hourly gauge precipitation in eastern China

Lingzhi Zhong [a,*], Zhiqiang Zhang [b], Lin Chen [c], Jinhong Yang [d], Fengling Zou [b]

[a] Chinese Academy of Meteorology and Science, Beijing, China
[b] National Meteorological Information Centre, China Meteorological Administration, Beijing, China
[c] National Satellite Meteorology Center, China Meteorological Administration, Beijing, China
[d] Meteorological Observation Center, China Meteorological Administration, Beijing, China

ARTICLE INFO

Article history:
Received 29 April 2015
Received in revised form 21 December 2015
Accepted 30 December 2015
Available online 8 January 2016

Keyword:
Quality control technique
Gauge rainfall
Weather radar
QPE application

ABSTRACT

The current real-time operational quality control method for hourly rain gauge records at meteorological stations of China is primarily based on a comparison with historical extreme records, and the spatial and temporal consistencies of rain records. However, this method might make erroneous judgments for heavy precipitation because of its remarkable inhomogeneous features. In this study, we develop a Radar Supported Operational Real-time Quality Control (RS_ORQC) method to improve hourly gauge precipitation records in eastern China by using Doppler weather radar data and national automatic rain-gauge network in JJA (i.e., June, July and August) between 2010 and 2011. According to the probability density function (PDF) and cumulative probability density function (CDF), we establish the statistic relationships between NSN precipitation records under 7 radar coverage and radar quantitative precipitation estimation (QPE). The other NSN records under 5 radar coverage are used for the verification. The results show that the correct rate of this radar-supported new method in judging gauge precipitation is close to 99.95% when the hourly rainfall rate is below 10 mm h^{-1} and is 96.21% when the rainfall intensity is above 10 mm h^{-1}. Moreover, the improved quality control method is also applied to evaluate the quality of provincial station network (PSN) precipitation records over eastern China. The correct rate of PSN precipitation records is 99.92% when the hourly rainfall rate is below 10 mm h^{-1}, and it is 93.33% when the hourly rainfall rate is above 10 mm h^{-1}. Case studies also exhibit that the radar-supported method can make correct judgments for extreme heavy rainfall.

1. Introduction

Precipitation plays an important role in weather and climate related studies, and especially the heavy rainfall may cause flash floods and consequent landslides, resulting in unexpected natural disasters. At present, rain gauge is a primary way to measure precipitation because it provides relatively accurate measurements at one site (Xie and Arkin, 1996; Adler et al., 2003; Harrison et al., 2009; Shen et al., 2010; Wang et al., 2012). The rain gauge measurements are also extensively employed to monitor heavy rainfall events. In China, more than 2000 rain gauge stations of the national station network (NSN) have been conducted with well-trained observers built since 1951. To further monitor local heavy rainfall events, more than 30,000 automatic rain gauges of the provincial station network (PSN) without personal supervisions have also been built since 2008. These rainfall measurements play important roles in monitoring local heavy rainfall events.

However, problems still exist in rain gauge records at PSN stations in China. For example, the tipping-bucket rain gauge was occasionally not able to tip over in time for heavy rainfall under the influence of strong winds; and vessels of rain gauges were occasionally shielded by trees, leaves, mud, and other things, or are artificially irrigated (Habib et al., 2001; Ciach, 2003; Upton and Rahimi, 2003; Huang, 2006). These may result in large errors in rain gauge measurements. Actually, both the NSN and PSN stations encounter the same problems. While the PSN stations are much annoyed by the problems because the NSN stations generally have artificial maintenance, and maintenance for PSN stations is less regular. Under some severe weather conditions with heavy rainfall occurring, it shows very weak precipitation from the gauge records. These wrong records could not usually be detected by present operational rainfall quality control method (Cong and Liu, 2011; Wang et al., 2015) especially for the PSN stations. All the false records were likely sent to users. Therefore, improving the quality control methods and techniques of rain gauge data is crucial for ignoring wrong records and confirming the data reliability.

In recent years, for the diversity of requirements to the quality of rainfall records, many quality control methods have been developed for the

* Corresponding author.
E-mail address: zhonglz@cams.cma.gov.cn (L. Zhong).

http://dx.doi.org/10.1016/j.atmosres.2015.12.016

Hydrological Data System (HADS), the River Forecast Center (RFCS), and the Weather Forecast System (WFOS) (Seo and Breidenbach, 2002; Nelson et al., 2008). The Global System Division (GSD) of NOAA Earth System Research Laboratory (ESRL) focuses on the good quality for long-term historical gauge records used in precipitation assimilation and verification (Tollerud et al., 2005; Kim et al., 2009). To remove false extreme precipitation records, the National Climate Data Center (NCDC) developed a quality control system according to the temporal continuity of rainfall records among different times at one station and the spatial consistency of hourly rainfall records between one station and the neighboring stations within 50 km (Kim et al., 2009). An operational procedure of quality control for rain gauge records has been built in the meteorological departments of Denmark, Finland, Iceland, Norway and Sweden (Rissanen et al., 2000; Vejen et al., 2002). This procedure includes three steps, i.e., the real-time quality control, the quality control of historical data, and the artificially interactive check.

Similar to the method developed by Kondragunta and Shrestha (2006), based on the temporal and spatial continuities of gauge rain records, an operational rainfall quality control (ORQC) system of the National Meteorological Information Center (NMIC) of China was also developed in 2010 (Ren and Xiong, 2007; Ren et al., 2010). The first step is to compare the real-time gauge records with the climatological extreme values (usually it is the maximum values in the statistical time period) for finding out the remarkable wrong records. The second step is to check the temporal and spatial consistencies between candidate rain gauge records and those at the neighboring stations and times. The third step is to further assure the gauge quality by manual method. There are three main ways for the "man–machine" interaction: a) when the forecasters detect extremely heavy rainfall records, they will contact with the local operators to check whether it's happening. b) In some cases, the local operator would record the weather information, especially the heavy rainfall events. c) Researchers will compare rainfall dataset with other information to reduce the error records. Although these manual method can improve the rainfall quality, it needs too much time and cost (Ren et al., 2010; Cong and Liu, 2011; Wang et al., 2015). Finally, the ORQC system marks "reliable" or "suspicious" or "false" records, which may help users utilize the data reasonably.

In the previous quality control methods, checking the temporal continuity and the spatial consistency is an important procedure, which is based on the assumption that the rainfall is relatively homogenous. However, heavy precipitation often occurs locally (Zhang et al., 2007; Moreau et al., 2009; Jaffrain and Berne, 2012; Qi et al., 2013; Gires et al., 2014). The rain record at one gauge station and one time has likely larger differences from those values in the adjacent areas and times. Therefore, the quality control methods only according to the homogeneity of rain gauge records in time and space occasionally make erroneous judgments (Cong and Liu, 2011). Due to these erroneous judgments, one local heavy rainfall events may be considered as a suspicious value or thrown away as an erroneous value (Kim et al., 2009).

To improve the quality control technique, therefore, the quantitative precipitation estimation (QPE) from weather radar reflectivity is often applied in judging the quality of rain gauge records (e.g., Kondragunta and Shrestha, 2006; Vasiloff et al., 2007). Techniques of applying radar QPE products to the quality control of rain gauge records have been developed (Kim et al., 2009). For example, in the United States, a comprehensive method of considering the spatial and temporal links between hourly radar QPE or multiple hourly QPE products and rain gauge records was developed by the National Severe Storms Laboratory (NSSL). In China, almost two hundred operational Doppler weather radars with a 10-cm (S band) or 5-cm (C band) wavelength have been established until 2012. They cover 16.9%, 38.3%, and 52.8% (27.1%, 59.8% and 76.8%) of land areas in China (eastern China) for heights of 1 km, 2 km, and 3 km away from the land surface, respectively (Wang et al., 2011). Thus, it is a great opportunity to apply these radar data for the quality control of rain gauge records over China.

In this study, to assure the timeliness of a real-time operational quality control system and to enhance the current real-time operational quality control technique, we establish a link between radar QPE products and hourly rain gauge records. Also, a new radar-supported quality control method is developed. The rest of this paper is organized as follows. The main features of datasets are described in Section 2. In Section 3, we introduce the strategies and principles of applying radar data in the quality control technique of rain gauge data. In Section 4, we assess the reliability of the radar-supported quality control technique and analyze some typical cases of heavy rainfall. Summary and further discussion and conclusion are provided in Section 5.

2. Data processing

2.1. Radar QPE

The S-band Doppler weather radars were mainly built across eastern China where the topography is relatively flat, while the C-band radars were mainly built in the other regions. Compared to the S-band radar, the C-band radar signal is attenuated greater for heavy rainfall and has a smaller coverage (Table 1). In China, the S-band radars from different manufacturers may be divided into three types, that is, SA, SB, and SC (Table 1) and they have differences in some radar parameters. Some parameters and hardware functions of the SA radars are similar to those of the US's WSR-88D and the software of the SA radars is the same as that of the WSR-88D. Key parameters of the SB radars are similar to those of the WSR-88D, but the receiver and antenna of the SB radars come from other manufacturers. Key parameters of the SC radars such as pulse width (1 μs) are different from those of the SA and SB radars (1.57 μs).

At present, there are 46 SA operation radars in eastern China (Fig. 1). After assessing the quality of the SA radar data and considering the relatively uniform distribution and low altitudes (<650 m) of SA radar stations across eastern China, we finally select 12 SA radars with good calibration quality at Guangzhou, Hefei, Hangzhou, Qinghuangdao, Shenzhen, Zhengzhou, Yancheng, Nanjing, Ningbo, Changsha, Shenyang, and Binzhou (shown in Fig. 1 and Table 2). All these radars are located in relatively flat terrain, which may reduce an impact of mountains on radar echoes. To further assess the quality of these ground-based radar data, following Liao et al. (2001), Wang et al. (2009) and Wen et al. (2011), we compare radar reflectivity at Nanjing, Hefei, Hangzhou, Ningbo, Changsha, and Zhengzhou stations with the space-boned precipitation radar (PR) of the Tropical Rainfall Measuring Mission (TRMM) in the 2011 and 2012 summer JJA (Table 3). Here these two data are interpolated on a horizontal resolution of 10 km and a vertical resolution of 500 m. An area-matching method and a temporal "window" of 10 min are used (Bolen and Chandrasekar, 2000; Heymsfield et al., 2000; Schumacher and Houze, 2000; Anagnostou et al., 2001; Wang et al., 2009). It is seen that the ground-based radar reflectivity is highly correlated with the PR, with correlation coefficients of 0.82–0.83. The mean absolute error is between 2.43 dBZ and 2.67 dBZ and the root mean square error (RMSE) is small (between 3.4 dBZ and 3.6 dBZ). These high correlations and small errors suggest the good consistency between the ground-based radar reflectivity and the TRMM PR, and the reliability of the former. The S-band radars complete one whole

Table 1
Parameters of different operational weather radars in China, in which S-band radars are divided into SA, SB, and SC types and C-band radars are divided into CC and CD types.

Name of radar type	SA	SB	SC	CC	CD
Frequency (GHz)	2.7–3.0	2.7–3.0	2.7–3.0	5.3–5.5	5.3–5.5
Beam width (°)	1	1	1	1	1
Antenna diameter (m)	11.8	11.9	11.8	4.5	4.5
Pulse width (μm)	1.57	1.57	1.0	0.8/1.0	2/2.5
Antenna gain (dB)	≥44	≥44	≥44	≥43	≥43
Peak power (KW)	≥650	≥650	≥650	≥250	≥250
City of manufacturer	Beijing	Nanjing	Chengdu	Anhui	Chengdu

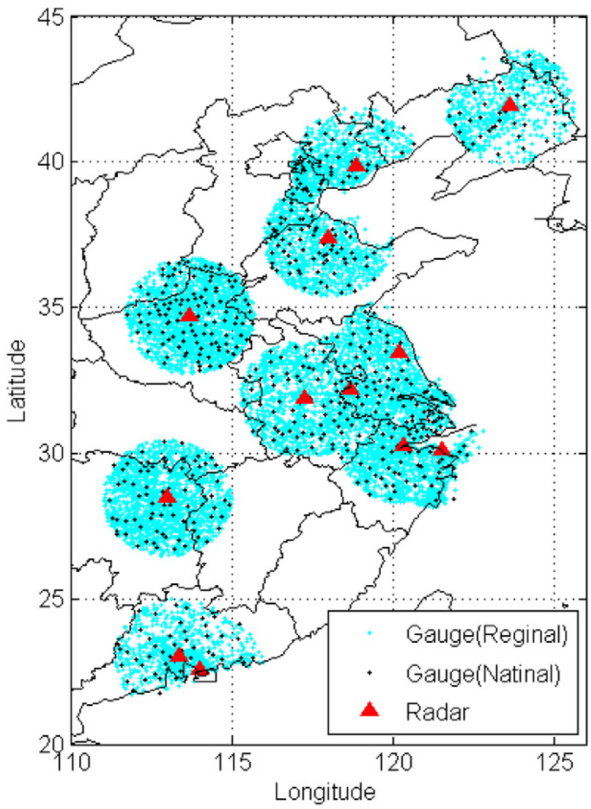

Fig. 1. Maps of the 12 S-band radar stations and the adjacent NSN and PSN rain gauge stations.

volume scan per six minutes, obtain 10 base reflectivity data per hour, and also suffer from different sources of errors, such as radar calibration, variation of the vertical reflectivity profile, bright band errors, attenuation, ground clutter, anomalous propagation, and wind drift errors (Harrison et al, 2000; Bringi et al, 2011; Rico-Ramirez and Cluckie, 2008; Rico-Ramirez, 2012). The quality control methods of radar data include the removals of noise and ground clutter as well as the quality control of the Doppler velocity (Oye et al., 1995). Following Xiao and Liu (2006), we firstly convert the original six-minute base reflectivity with the polar coordinates into the three-dimensional Cartesian coordinate data with a horizontal resolution of 1 km and a vertical resolution of 0.5 km (1 km) below the height of 8 km height (above the height of 8 km) above ground level. Under the influence of wind speed, evaporation, and radar beam blocking, the radar QPE is often underestimated (Zhang et al., 2001). To reduce such an underestimation, for each volume gridded value, we choose the reflectivity (or maximum reflectivity) at the lowest level (or in the vertical direction) when the

Table 2
Information of 12 S-band radars in eastern China ("*" stands for establishing statistical relationships; "☆" stands for a comparison with TRMM-PR radar).

Radar name	Latitude (°)	Longitude (°)	Height (m)
*Guangzhou	23.00	113.36	181
☆Nanjing	32.19	118.70	138
☆*Hefei	31.87	117.26	166
*Yancheng	33.43	120.20	28
☆Hangzhou	30.27	120.34	96
☆*Ningbo	30.07	121.51	458
☆Changsha	28.46	113.01	630
*Shenzhen	22.54	114.01	149
Shenyang	41.93	123.65	299
☆*Zhengzhou	34.70	113.69	202
Binzhou	37.37	118.00	70
*Qinhuangdao	39.88	118.88	114

Table 3
Correlation coefficient (R), bias, mean absolute error (MAE), and root mean square error (RMSE) between SA radars and TRMM PR over eastern China, in which height stands for the distance above the ground level (AGL) and points stand for matching samples.

Height (km)	R	Bias	MAE	RMSE	Points
2	0.82	−4.08	2.67	3.61	4445
3	0.82	−3.41	2.54	3.48	11,066
4	0.82	−3.26	2.50	3.42	43,212
5	0.83	−3.34	2.43	3.39	86,437

reflectivity is ≥15 dBZ (or <15 dBZ). In this way, we generate the "mixed height radar reflectivity", which is similar to the hybrid scan reflectivity used in NSSL. Secondly, according to the methods of Steiner and Yuter (1995) and Zhong et al. (2007), we only consider the mixed height radar reflectivity for convective and stratiform cloud types. The threshold value of radar reflectivity for one convective cell is set to be 38 dBZ according to the features of convective rainfall in eastern China (Zhong et al., 2007). Thirdly, we calculate the accumulated rainfall within 6 min for convective and stratiform cloud types by means of a Z–R relationship as follows (Zhang et al., 2001; Zhang et al., 2008).

$$\text{For convective cloud,}\quad Z = 300R^{1.4}, \tag{1}$$

$$\text{For stratiform cloud,}\quad Z = 200R^{1.6}. \tag{2}$$

Here Z is the radar reflectivity ($mm^6\,m^{-3}$); and R is the rainfall intensity ($mm\,h^{-1}$). Finally, the hourly accumulated QPE is an arithmetic sum of six-minute rainfall in 1 h. However, the radar data are occasionally missing. In this case, when there are six or more missing radar data in 1 h, the mean value in this period is defined as the maximum value, being used to calculate the hourly accumulated rainfall. The radar QPE data used in this study are not corrected by rain gauge data, dual polarization radar data, and vertical profile of reflectivity.

Because the latitudes and longitudes of rain gauge stations are not always corresponded to those of radar grid data, we select 9 directions (including east, west, south, north, northeast, northwest, southeast, and southwest) within a box of 3 km × 3 km with one gauge station as the center. These nine lattices are matched with the three-dimensional radar grid based on the neighboring method. Moreover, mark the value which is closest to the gauge rainfall record within the box of 3 km × 3 km area (totally nine values) as "R_r". Meanwhile, the maximal value of radar QPE within this box is marked as R_{r_max}.

2.2. Rain gauge data

The NSN rain gauge stations are supervised by meteorologists and each NSN rainfall record archived at the National Meteorological Information Center of China is carefully checked again. When some erroneous NSN records are detected, they will be corrected (Ren et al., 2010). Thus the quality of these checked NSN data is generally good and they may be used to assess the ability of our quality control technique. In the present study, we use the NSN hourly automatic rain gauge records near 12 S-band radar stations (Fig. 1) during the 2010 and 2011 summers (JJA) to statistically establish relationships between rain gauge records and radar QPE. For these NSN stations during the 2010 and 2011 summers, we obtain 898,142 hourly rainfall records. Among them, 513,570 records are used for determining the thresholds and the other 384,572 records are used for validation of the method. Moreover, 1,601,695 PSN hourly rainfall records near five radar stations (Nanjing, Ningbo, Changsha, Shenyang, and Binzhou) (Fig. 1) are also used.

3. Algorithm of the radar-supported QC method

According to the technical report from the National Meteorological Center of China (NMCC, 2011), one wrong judgment for true heavy precipitation will result in a lot of loss. In this study, we focus on zero and

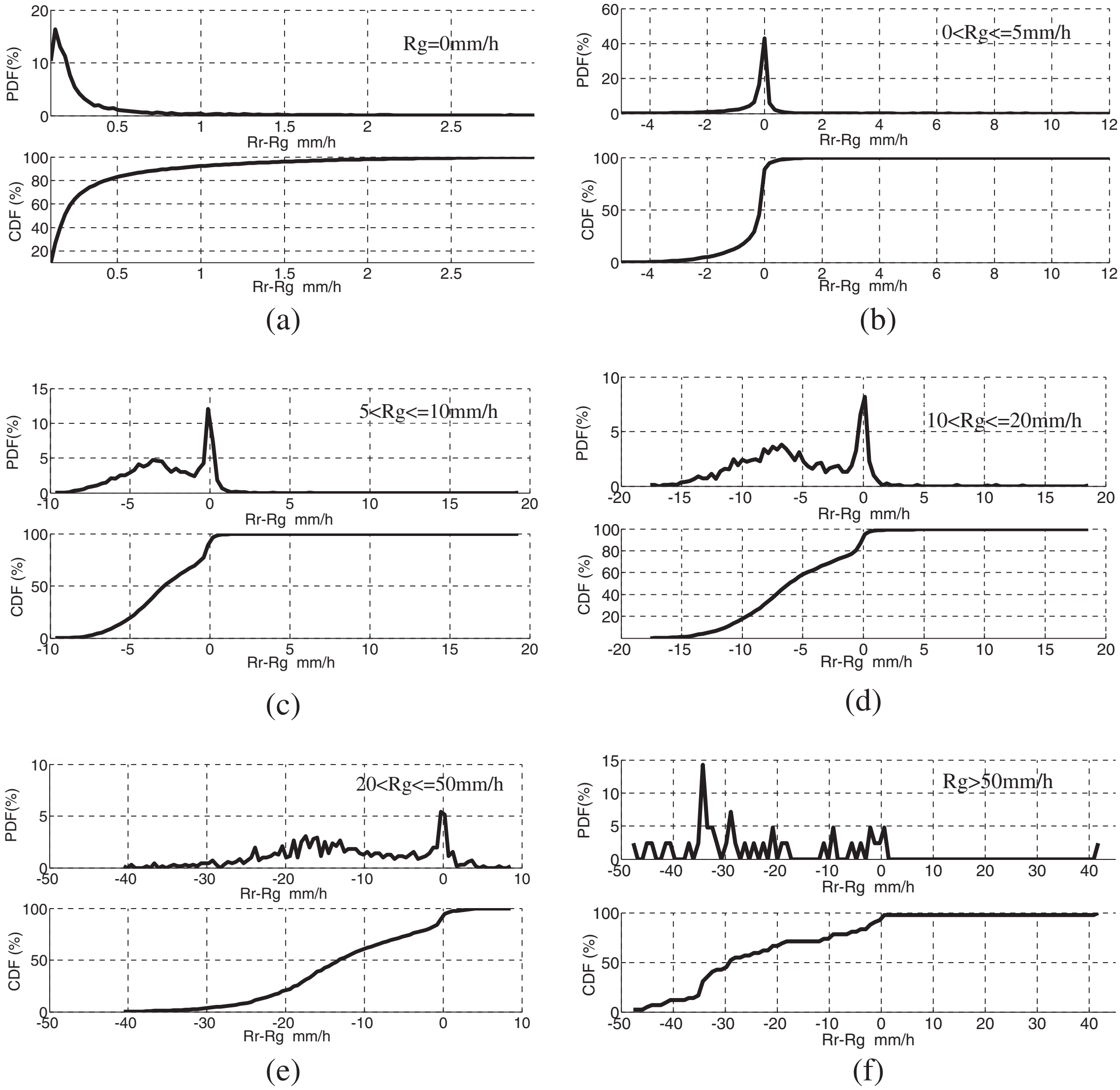

Fig. 2. Probability density distribution (PDF) and accumulative PDF (CDF) of difference (ΔR) between hourly gauge record and radar QPE for different hourly rain grades.

Table 4
Criterions for different R_g grades by considering multiple errors.

R_g grades ($mm\ h^{-1}$)	Strict criteria of ΔR ($mm\ h^{-1}$)	Relaxed criterions of ΔR ($mm\ h^{-1}$)
$R_g = 0$	$\Delta R \in [0, 2.5]$	When $\Delta R > 5.0$, R_g is wrong When $3.7 < \Delta R \le 5.0$, R_g is suspicious When $\Delta R \le 3.7$, R_g is right
$0 < R_g \le 5$	$\Delta R \in [-4.0, 2.0]$	When $\Delta R > 7.0$, R_g is wrong When $5 < \Delta R \le 7.0$, R_g is suspicious When $\Delta R \le 5$, R_g is right
$5 < R_g \le 10$	$\Delta R \in [-7.5, 5.0]$	When $\Delta R > 15.0$ or $\Delta R \le -8.0$, R_g is wrong When $11.0 < \Delta R \le 15.0$, R_g is suspicious When $-8.0 < \Delta R \le 11.0$, R_g is right
$10 < R_g \le 20$	$\Delta R \in [-15.0, 20.0]$	When $\Delta R > 40.0$ or $\Delta R \le -15.5$, R_g is wrong When $32.0 < \Delta R \le 40.0$, R_g is suspicious When $-15.5 < \Delta R \le 32.0$, R_g is right
$20 < R_g \le 50$	$\Delta R \in [-30.0, 10.0]$	When $\Delta R > 85.0$ or $\Delta R \le -45.0$, R_g is wrong When $50.0 < \Delta R \le 85.0$, or $-45.0 < \Delta R \le -35.0$, R_g is suspicious When $-35.0 < \Delta R \le 50.0$, R_g is right
$R_g > 50$	$\Delta R \in [-47.0, 40.0]$	When $R_g \ge 70$ and $R_{max} \ge 34$, R_g is right When $60 \le R_g < 70$ and $R_{max} \ge 25$, R_g is right When $50 < R_g < 60$ and $R_{max} \ge 12$, R_g is right When $10 < R_{max} < 12$, R_g is suspicious For other cases, R_g is wrong

heavy gauge rainfall records (R_g), dividing into six types, that is, $R_g = 0\ mm\ h^{-1}$, $0 < R_g \le 5\ mm\ h^{-1}$, $5 < R_g \le 10\ mm\ h^{-1}$, $10 < R_g \le 20\ mm\ h^{-1}$, $20 < R_g \le 50\ mm\ h^{-1}$, and $R_g > 50\ mm\ h^{-1}$.

To apply radar QPE to the quality control of gauge rainfall, a statistical relationship needs to be established between QPE and gauge rainfall. Above of all, 513,570 hourly rainfall records at NSN stations are divided into six groups. They are $R_g = 0\ mm\ h^{-1}$ (with the sample number of 442,267), $0 < R_g \le 5\ mm\ h^{-1}$ (38,845), $5 < R_g \le 10\ mm\ h^{-1}$ (3470), $10 < R_g \le 20\ mm\ h^{-1}$ (2824), $20 < R_g \le 50\ mm\ h^{-1}$ (721), and

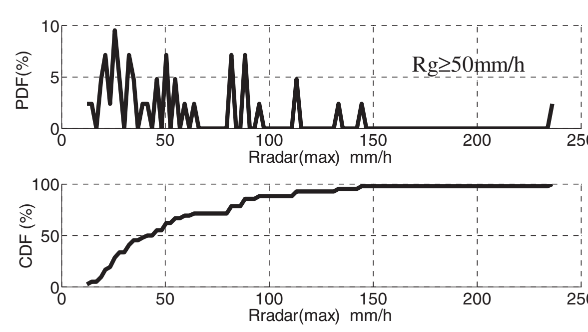

Fig. 3. PDF and CDF of maximum radar QPE when $R_g \ge 50\ mm\ h^{-1}$.

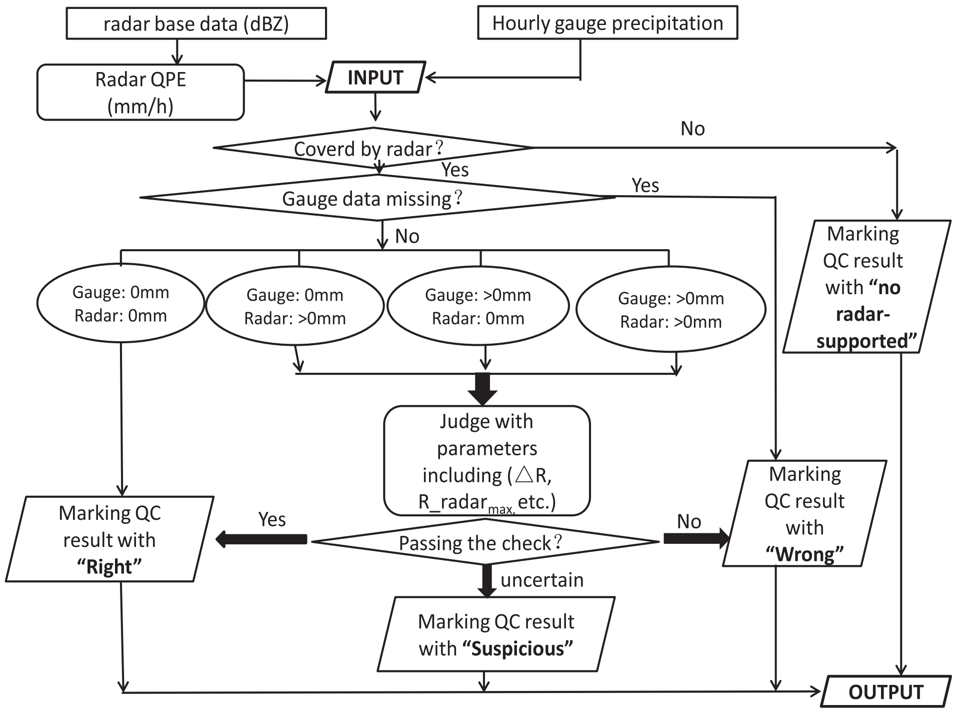

Fig. 4. Flowchart of the radar-supported quality control for hourly gauge rainfall.

$R_g > 50$ mm h^{-1} (43). For each group, the threshold of ΔR is determined by analyzing both the probability density function (PDF) and the cumulative PDF (CDF) of ΔR, in which ΔR is defined as a difference ($\Delta R = R_r - R_g$) between R_r and R_g, and R_r is for radar QPE. Using radar QPE data at Guangzhou, Hefei, Hangzhou, Qinghuangdao, Shenzhen, Zhengzhou, and Yancheng stations and rainfall data at the 568 adjacent NSN stations, we establish one statistical model. The other five radar QPE data at Nanjing, Ningbo, Changsha, Shenyang, and Binzhou stations are used to validate the reliability of the model.

Fig. 2a shows the curves of PDF and CDF of ΔR for $R_g = 0$. It is seen that when $R_g = 0$, the PDF of ΔR shows one peak near 0.05 mm h^{-1}. The CDF rapidly increases with ΔR, arriving at 99.8% near 2.5 mm h^{-1}. The sample number with rainfall between 0 and 2.5 mm h^{-1} accounts for 99.8% of the total sample number (442,267). This indicates that when $R_g = 0$, the 99.8% of ΔR varies between 0 and 2.5 mm h^{-1}. In this study, therefore, 2.5 mm h^{-1} is defined as the value of ΔR_base for $R_g = 0$. When ΔR is between 0 and 2.5 mm h^{-1}, $R_g = 0$ is judged to be “right”; otherwise, $R_g = 0$ is judged to be “suspicious”. The previous research has shown that for heavy rainfall the mean error of radar QPE in China is often near 40%, even up to 100%–120% (Zhang et al., 2001). Considering errors in radar QPE, location matching between rain gauge records and radar grid data, and mall scale rainfall variability etc. (see Sections 1 and 2), we relax the above threshold determined only by the quantile of CDF. The thresholds for other grades of gauge rain records are similarly determined, in which all samples are chosen for $R_g > 50$ mm h^{-1} (due to the small sample number for this grade) and the 99% quantile is chosen for other rain grades. Finally we use three markers (“right”, “suspicious”, and “wrong”) to indicate the result of the rainfall quality control. The relaxed thresholds are given as follows. For $R_g \le 20$ mm h^{-1}, when $\Delta R > \Delta R\_base + 100\% \times R_g$, R_g is judged to be “wrong”; when $\Delta R \le \Delta R\_base + 60\% \times R_g$, R_g is judged to be “right”; and when $(\Delta R\_base + 60\% \times R_g) < \Delta R \le (\Delta R\_base + 100\% \times R_g)$, R_g is judged to be “suspicious”. For $R_g > 20$ mm h^{-1}, when $\Delta R > \Delta R\_base + 150\% \times R_g$, R_g is judged to be “wrong”; when $\Delta R \le \Delta R\_base + 80\% \times R_g$, R_g is judged to be “right”; when $(\Delta R\_base + 80\% \times R_g) < \Delta R \le (\Delta R\_base + 150\% \times R_g)$, R_g is judged to be “suspicious”. Finally, we get the thresholds, that is, “$R_g = 0$” is accepted as a “right” value when ΔR is between 0 and 3.7 mm h^{-1}, as a “suspicious” value when ΔR is between 3.7 mm h^{-1} and 5 mm h^{-1}, and as a “wrong” value when ΔR is greater than 5 mm h^{-1}. Similarly, we also analyze Fig. 2b to f and then obtain the thresholds for other rainfall grades (see Table 4). To test the sensitivity of the results to these thresholds, we also slightly adjust these threshold values. For example, we choose [0, 3] at the 99.85% quantile and [0, 5] at the 99.93% quantile for $R_g = 0$ [−3, 1] at the 98.7% quantile and [−5, 5] at the 99.6% quantile for $0 < R_g \le 5$, and so on.

In Fig. 2, with an increase of R_g, the underestimation of R_r is more remarkable, PDF of ΔR has more than one peaks as well as their values decrease. The reason for the phenomenon of various peaks may be because the lack of samples. In the future, this needs to be further researched. For example, when $R_g > 50$ mm h^{-1}, PDF of ΔR has peaks of about 15% at −34 mm h^{-1}, about 7% at −29 mm h^{-1}, and about 5% at −21 mm h^{-1}, −9 mm h^{-1}, and −2 mm h^{-1}, which indicates a

Table 5
Evaluation of the RS_ORQC method with the NSN rain records, in which *r*, *w*, and *s* are for N_r/N_t, N_w/N_t, and N_s/N_t, respectively.

R_g (mm h^{-1})	Samples	N_r/r	N_w/*w*	N_s/s
$R_g = 0$	336,952	336827/99.96%	93/0.03%	32/0.01%
$0 < R_g <= 5$	40,938	40937/99.99%	0/0	1/0.01%
$5 < R_g <= 10$	3724	3666/98.44%	57/1.53%	1/0.03%
$10 < R_g <= 20$	2044	1976/96.67%	66/3.23%	2/0.1%
$20 < R_g <= 50$	865	821/94.91%	29/3.35%	15/1.74%
$R_g > 50$	49	46/93.88%	1/2.04%	2/4.08%

Table 6
The “wrong”, “suspicious”, and “right” numbers of judging 71 typical rainfall cases at the PSN stations by the ORQC and RS_ORQC methods.

ORQC	RS_ORQC		
	Wrong	Suspicious	Right
Wrong	0	0	1
Suspicious	25	5	0
Right	40	0	0

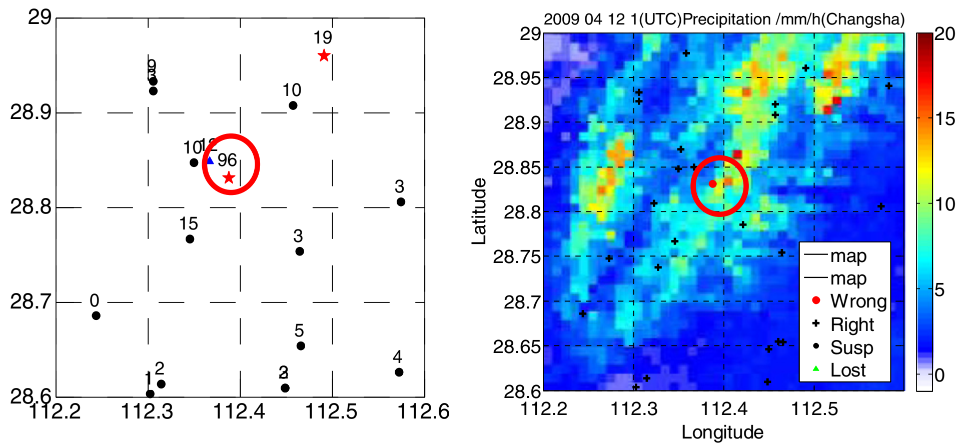

(a) (b)

Fig. 5. (a) Distribution of PSN hourly rainfall in Changsha city of Hunan Province at 0100 UTC on April 12th, 2009, in which the red star indicates station P2667; and (b) same as in (a) but for the radar QPE, in which the red dot indicates station P2667.

large varying range of ΔR for much heavy hourly rainfall. In this case, our analysis further shows that when the above thresholds are used, some real heavy rainfall records are possibly misjudged to be "wrong". Thus, for $R_g > 50$ mm h^{-1}, we further consider the maximum value of R_r (R_{r_max}) within a box of 3 km × 3 km around a gauge station. Fig. 3 shows the PDF and CDF of R_{r_max} for $R_g > 50$ mm h^{-1}. It is seen that the minimum value of R_{r_max} is near 12 mm h^{-1}. When the minimum value of R_{r_max} is >12 mm h^{-1}, the heavy rainfall record more than 50 mm h^{-1} is further judged to be "right". Similarly, we may get the thresholds of R_{r_max} for 50 mm h^{-1} < R_g ≤ 60 mm h^{-1}, 60 mm h^{-1} < R_g ≤ 70 mm h^{-1}, and R_g > 70 mm h^{-1}, respectively (Table 4). Since there is a small number of samples when R_g > 50 mm h^{-1}, its thresholds need to be further verified by using more samples.

Based on the above method, we design a quality control flowchart (Fig. 4). Firstly, we input radar QPE (calculated from radar base data per 6 min) and hourly accumulated gauge rainfall data (calculated from minute-scale rainfall records) into the radar-supported ORQC (hereafter RS_ORQC) system. If one rain gauge record exists/is covered by radar QPE, we compare the rain gauge record with radar data; otherwise, the rain gauge record is judged to be "wrong"/"no radar-supported" is marked, and then the procedure of the quality control ends. When both rain gauge records and radar QPE are indicated by "zero", rain gauge records are judged to be "right" and then the procedure ends; otherwise, a more complicate judgment will be performed (shown in Table 4). We finally mark the rainfall quality as a "right" value, or a "suspicious" value, or a "wrong" value. In the following section, we evaluate this new quality control method using the other five radar data (at Nanjing, Ningbo, Changsha, Shenyang, and Binzhou stations) and their nearby NSN and PSN gauge rain records.

4. Evaluation, case study, and application of the radar-supported ORQC method

4.1. Evaluation with NSN rainfall data

To assess the ability of the RS_ORQC method developed in Section 3, utilizing radar QPE products at Nanjing, Ningbo, Changsha, Shenyang, and Binzhou stations and hourly gauge rain data (checked by meteorologists and considered to be reliable records) at 379 NSN stations in the 2010–2011 summers, we evaluate the ability of the RS_ORQC method. The total sample number (N_t) of hourly rain record is 384,572. The number of "right"/"suspicious"/"wrong" R_g is represented by "N_r"/"N_s"/"N_w", in which N_t is an arithmetic sum of N_r, N_s, and N_w. In this study, we use "right", "suspicious", and "wrong" rates to evaluate the ability of the quality control method.

Table 5 shows the assessment result. It is seen that for R_g = 0 mm h^{-1}, 99.96% rain gauge records are judged to be "right" by the RS_ORQC method, which shows that the RS_ORQC method can correctly judge the 99.96% NSN rain gauge records, and only 0.03% and 0.01% records are misjudged to be "wrong" and "suspicious", respectively. For 0 mm h^{-1} < R_g ≤ 5 mm h^{-1}, 5 mm h^{-1} < R_g ≤ 10 mm h^{-1}, and 10 mm h^{-1} < R_g ≤ 20 mm h^{-1}, more than 96% records are judged to be "right". For more than 50 mm h^{-1} heavy rainfall, the almost 94% records are judged to be "right". These correct rates show that for different rain grades, at least 94% reliable NSN rain gauge records are also judged to be "right". When we slightly adjust the thresholds (see Section 3), the "right" rates do not remarkably change. This suggests that the improved quality control method is reliable for different NSN rainfall rates. We further compare with the results of the NMIC operational ORQC method (Ren et al., 2010). According to their study, for NSN stations, the "right" and "suspicious" rates of the ORQC method are about 93.8% and 6.1% during 2006–2009, respectively. It is evident that the "right" rates of the ORQC method are smaller compared to our method. This result suggests a higher misjudgment rate of the ORQC method. Therefore, only using the consistencies of rain gauge records in time and space is poorer in judging the quality of heavy rainfall. The ORQC method enhances the rates of correct judgment.

4.2. Case study of PSN rainfall records in flood season

We also use some checked (by meteorologists) PSN precipitation cases to assess the RS_ORQC method. Using the 71 typical rainfall records (misjudged by the ORQC method) during the 2010–2011 summers provided by the NMCC (2011), we compare the results of the

Table 7
The ORQC and RS_ORQC methods at stations P2667 and B2423, in which "actual" stands for checked precipitation by meteorologists '×' for 'wrong', '?' for 'suspicious', and '√' for 'right'; and R_radar_{min}, R_radar_{mean}, and R_radar_{max} are for the minimum, mean, and maximum values of radar QPE, respectively.

Station code	R_g (mm h^{-1})	ORQC/(actual)	RS_ORQC	R_radar_{min} (mm h^{-1})	R_radar_{mean} (mm h^{-1})	R_radar_{max} (mm h^{-1})
P2667	96.0	?/(×)	×	4.3	15.7	17.5
B2423	157	×/(√)	√	151.0	158.1	161.1

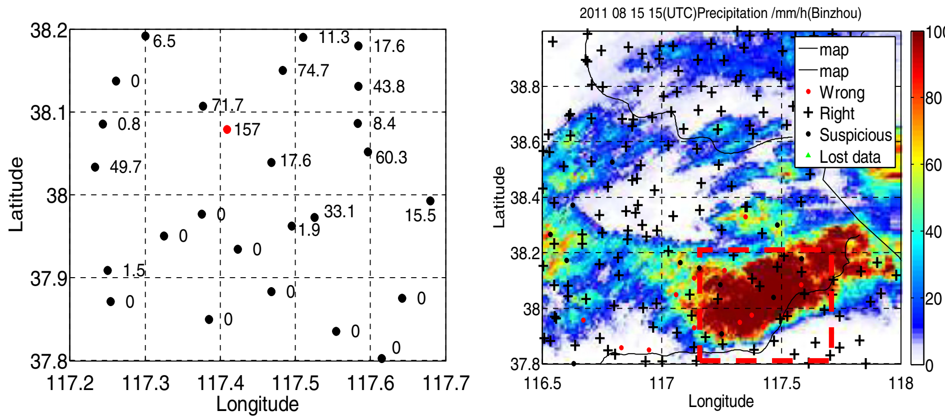

(a) (b)

Fig. 6. (a) Distribution of hourly rain gauge records in Binzhou city of Hebei Province at 1500 UTC on August 15th, 2011, in which the red dot indicates station B2423; and (b) same as in (a) but for the radar QPE, in which the red box is for the area in (a).

ORQC and RS_ORQC methods (Table 6). Among 71 rainfall records, 40 of them are judged to be "right" by the ORQC who are judged to be "wrong" in the RS_ORQC methods. During the records which were judged to be "suspicious", 25 of them are judged to be "wrong" and 5 of them are marked as "suspicious". Only one record marked as "wrong" in ORQC method is judged as "right" in RS_ORQC. Thus, the RS_ORQC method shows a good performance in qualifying these 71 cases.

a) Isolated false extreme precipitation

The hourly rainfall of 96 mm h^{-1} was recorded by station P2667 in Hunan Province at 0100 UTC on April 12th, 2009 (Fig. 5a). Because this value was obvious higher than rainfall at the surrounding stations, the rainfall of 96 mm h^{-1} was judged to be "suspicious" in the real-time ORQC system. However, this record is judged to be "wrong" by RS_ORCS method. In fact, the investigation of meteorologists showed that the rainfall record was zero at that time, and the amount of its daily rainfall is far less than 96 mm/h. It is seen in Fig. 5b that the P2667 station is located within the red circle with QPE values between 4.3 mm h^{-1} and 17.5 mm h^{-1} (Table 7). Even though one reasonable error of radar QPE is considered, the gauge rainfall of 96 mm h^{-1} is also not supported by radar QPE. Thus this value is judged to be "wrong" by radar QPE.

b) Isolated true extreme precipitation

Fig. 6a shows hourly rain records in Binzhou city of Hebei Province at 1500 UTC on August 15th, 2011. In this figure, there were an hourly rainfall value of 157 mm h^{-1} at station B2423 and rainfall values between 70 mm h^{-1} and 80 mm h^{-1} at its adjacent stations. In the ORQC method, 157 mm h^{-1} is judged to be "wrong" because of a remarkable inhomogeneous feature in space. But, the radar QPE at Binzhou station (Fig. 6b) clearly indicates a regional mean value of 158 mm h^{-1} at station B2423, with a minimum value of 151 mm h^{-1} and a maximum value of 161 mm h^{-1} within a box of 3 km × 3 km over station B2423 and a regional mean value above 90 mm h^{-1} at the adjacent areas (Table 7). Thus, 157 mm h^{-1} at station B2423 is judged to be "right" in the RS_ORQC method. Afterwards, our visit to some meteorologists at station B2423 and its adjacent stations also verified that an exceptional "downpour" rainfall (without hail) did occur at that time, resulting in a serious disaster and economic loss.

c) Longtime false extreme precipitation of single station

Table 8
Quality control results at station M5401 from 21 to 22, July, 2011 by the ORQC and RS_ORQC methods, in which "actual" is for checked precipitation by meteorologists; and '×' is for 'wrong', '?' is for 'suspicious', and '√' is for 'right'.

Time (UTC)	R_g (mm h^{-1})	ORQC/(actual)	RS_ORQC
00:00	0.0	√/(√)	√
01:00	0.0	√/(√)	√
02:00	10.8	?/(×)	×
03:00	12.6	?/(×)	×
04:00	1.2	√/(√)	√
05:00	5.3	√/(×)	×
06:00	2.3	√/(√)	√
07:00	13.9	?/(×)	×
08:00	3.6	√/(×)	?
09:00	Missing	–	–
10:00	2.8	√/(√)	√
11:00	16.2	?/(×)	×
12:00	14.4	?/(×)	×
13:00	4.4	√/(√)	√
14:00	0	√/(√)	√
15:00	24.6	?/(×)	×
16:00	6.2	√/(×)	×
17:00	6.4	√/(×)	×
18:00	19.6	? /(×)	×
19:00	2.4	√/(√)	√
20:00	9.6	? /(×)	×
21:00	3.7	√/(√)	√
22:00	8.3	? /(×)	×
23:00	7.2	? /(×)	×
00:00	9.8	? /(×)	×

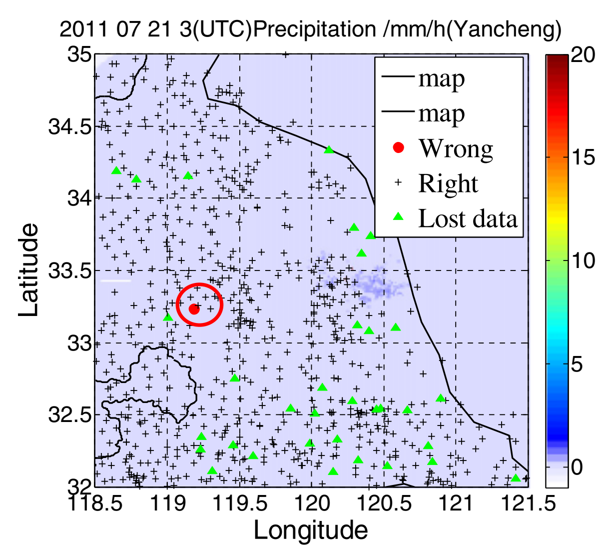

Fig. 7. Distributions of the radar QPE (see the color bar) at Yancheng radar station at 0300 UTC on July 21st, 2011 and results of the quality control at PSN gauge rainfall. The red circle indicates station M5401.

Table 9
Same as Table 7 but at Zhengzhou radar stations on July 7th, 2011.

R_g (mm h^{-1})	ORQC / (actual)	RS_ORQC	R_radar_{min} (mm h^{-1})	R_radar_{mean} (mm h^{-1})	$R\_radar_{nearest}$ (mm h^{-1})
0.0	√/(×)	×	17.3	19.8	12.1
0.0	√/(×)	×	9.0	10.2	8.5
68.7	?/(×)	×	0.2	0.0	0.0
108.4	?/(×)	×	0.0	0.0	0.0
114.7	?/(×)	×	0.0	0.0	0.0
100.3	?/(×)	×	0.0	0.0	0.0
98.0	?/(×)	×	0.0	0.0	0.0
142.7	?/(×)	×	0.0	0.0	0.0
5.6	?/(×)	×	0.0	0.0	0.0

Table 10
Evaluation of the PSN gauge rain quality by the RS_ORQC method, in which *r*, *w*, and *s* are for N_r/N_t, N_w/N_t, and N_s/N_t, respectively.

R_g (mm h^{-1})	Samples	N_r/r	N_w/w	N_s/s
$R_g = 0$	1,121,380	1120601/99.93%	183/0.02%	596/0.05%
$0 < R_g <= 5$	408,365	408197/99.95%	138/0.03%	30/0.02%
$5 < R_g <= 10$	42,771	42481/99.32%	288/0.67%	2/0.01%
$10 < R_g <= 20$	20,289	19086/94.07%	1173/5.78%	30/0.15%
$20 < R_g <= 50$	8463	7756/91.65%	435/5.14%	272/3.21%
$R_g > 50$	427	385/90.16%	40/9.37%	2/0.47%

At one station, some "false" heavy precipitation records occasionally occur continuously in one period. For example, at station M5401 of Yancheng in Jiangsu Province, the daily accumulative precipitation was higher than 128 mm h^{-1} from 0000 UTC on July 21st to 0000 UTC on July 22nd, 2011, with the maximum hourly precipitation record of 24.6 mm h^{-1} (Table 8). In the ORQC system, 13 (11) hourly rainfall records were judged to "right" ("suspicious"). On the map of radar QPE, however, there were no large radar QPE values near station M5401 in this period (see Fig. 7). Therefore, the result of the RS_ORQC method shows 9 "right", 14 "wrong", and 1 "suspicious" records. The investigation of meteorologists showed that the 24-h accumulated precipitation amount near station M5401 was less than 1 mm. At one single station in Zhengzhou Province, there was one extreme precipitation record of as high as 148.4 mm h^{-1} on July 7th, 2011, with the 24-h accumulated precipitation amount of >700 mm (Table 9). For the ORQC method, 7 gauge rainfall records are judged to be "suspicious" and two zero records are judged to be "right" (Table 9). For the RS_ORQC method, all these records are judged to be "wrong". In fact, there was basically no heavy precipitation at this station. These results exhibit that the RS_ORQC method remarkably improves the accuracy of the ORQC method.

4.3. Evaluating the quality of rainfall at PSN stations

Here we further apply the RS_ORQC method in assessing the quality of 1,603,250 PSN rainfall records in Guangzhou, Nanjing, Hangzhou, and Hefei in JJA (June, July and August) of during 2010 and 2011. An assessment by the ORQC method indicates that 99.9% records (1,601,695) are judged to be "right". However, the result of the RS_ORQC method shows that 0.2% of those "right" records in ORQC method are judged to be "suspicious" or "wrong" (see Fig. 8 and Table 10). The rates of "right", "suspicious", and "wrong" records are 99.80%, 0.14%, and 0.06%, respectively. The rate of "right" records decreases with an increase of the rainfall intensity., the rate of "right" records is 94%, 91.65%, and 90.16% for 10 mm $h^{-1} < R_g \le 20$ mm h^{-1}, 20 mm $h^{-1} < R_g \le 50$ mm h^{-1}, and $R_g > 50$ mm h^{-1} respectively. These features are similar to the NSN records. For all grades of the PSN rainfall, the "right" rates exceed 90%, which suggests that the PSN rainfall quality is generally good, but slightly lower compared to that of the NSN. Fig. 8 gives the "wrong" and "suspicious" rates of between the ORQC and RS_ORQC methods in judging NSN and PSN gauge rainfall data for different rainfall intensity. In this figure, when $R_g = 0$, the "right" rate is almost 100% for the ORQC method. With an increase of the rainfall intensity, however, the mean rates of both "wrong" and "suspicious" records of the ORQC method quickly increase. For example, for $R_g \geqq 50$ mm h^{-1}, the rate of both "wrong" and suspicious records is larger than 70%, which means nearly more than 2/3 rainfall dataset couldn't be used. In another way, the "right" rates of the ORQC method are much smaller compared to RS_ORQC method. It's evident that ORQC method shows a poorer judgment for heavy rainfall relative to RS_ORQC method, and the rate of the "wrong" and "suspicious" records is much more reasonable for RS_ORQC method than ORQC method. In another way, from the "wrong and suspicious rates" it is evident that the PSN stations are actually affected by a poor maintenance, and an improved real-time quality control system should be applied as well as better maintenance established for them.

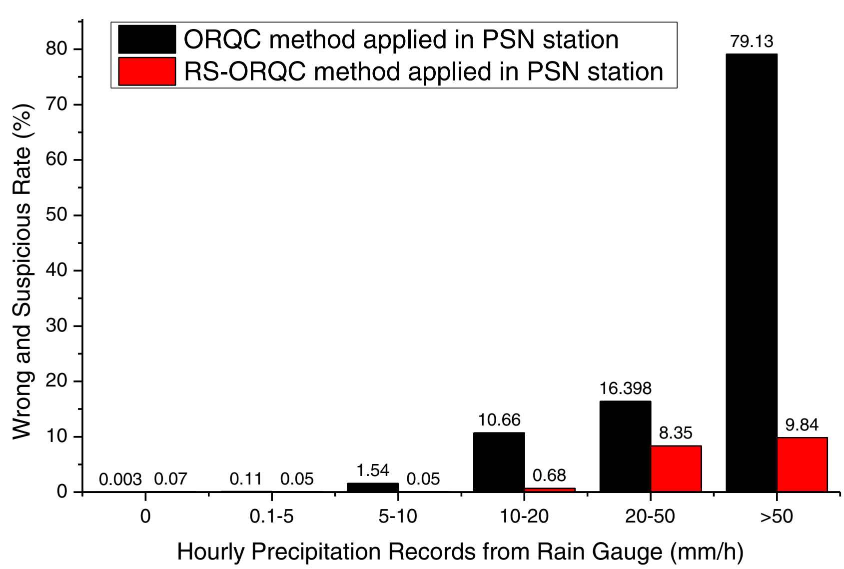

Fig. 8. "Wrong" and "suspicious" rates of the ORQC and RS_ORQC methods in judging NSN and PSN gauge rainfall data for different rainfall grades. The black bar stands for ORQC method, and the red one stands for RS_ORQC method..

5. Conclusions and discussions

Using the Doppler weather radar data and the adjacent automatic rain gauge data over eastern China in JJA between 2010 and 2011, a real-time radar-supported method is developed for controlling hourly gauge rainfall data quality. It is called the Radar-Supported Operational Real-time Quality Control method (RS-ORQC). First, the statistical relationships are established between rain gauge records and seven radar QPE data, in which the PDF and CDF of differences between radar QPE and gauge records are used to determine the thresholds for judging the quality of gauge rain records for six rain grades. Because of multiple errors in radar QPE, location matching between gauge and radar grid data, and mall scale rainfall variability etc., these thresholds are relaxed for each grade. The final index of RS_ORQC is marked with "right", or "wrong", or "suspicious".

Using the radar QPE data at Nanjing, Ningbo, Changsha, Shenyang, and Binzhou stations and 384,572 checked hourly gauge rain records at 379 adjacent NSN stations, the ability of the RS_ORQC method is evaluated. The result shows that the total "right" rate accounts to 99.92%. It is 99.96% when $R_g = 0$ mm h^{-1}, >96% when $0 < R_g \le 5$ mm h^{-1}, 5 mm h^{-1} < $R_g \le 10$ mm h^{-1}, and 10 mm h^{-1} < $R_g \le 20$ mm h^{-1}, and about 94% when $R_g > 50$ mm h^{-1}. All these results exhibit the high consistency between RS_ORQC method and the NSN gauge records. However, the "right" rate of the present ORQC method is lower than 94% (Ren et al., 2010). Moreover, the comparisons between gauge rain records and radar QPE data are done for typical cases of heavy rainfall. Some extreme heavy rain records were also successfully judged by the RS_ORQC method.

Moreover, the RS_ORQC method is applied for assessing the quality of the PSN rainfall in Guangzhou, Nanjing, Hangzhou, and Hefei cities during the 2010–2011 summers. The "right" rate of the PSN rain data is 99.96%, the "wrong" rate is 0.01%, and the "suspicious" rate is 0.03%. These results suggest that the PNS rain gauge records during the 2010 and 2011 summers are generally convinced. However, Ren et al. (2010) showed that the "right" rate of hourly gauge records in 2006–2009 is 98.6%, which underestimates the correct rate of the PSN gauge data, especially in the extreme precipitation events.

In the present study, we merely use SA weather radar data for the quality control of rain gauge records and consider liquid precipitation in the algorithm over eastern China. It is not suitable for hail phenomena events. When developing the radar-supported quality control of gauge rain records, we have to consider the differences of these radar QPE products, e.g. calibration biases, Z–R relationships for various rain types. In another way, the space-boned radar observation (e.g. PR and DPR) are now developed, which may greatly reduce the topographic effects on radar echoes, and may introduce more information about the hydrometer particle phases. All of these detectors will be useful to develop an improved quality control method for mountainous areas.

Acknowledgments

We thank Professors Xiaoding Yu, Anyuan Xiong, Ping Zhao, Yuchun Gao, Zhihua Ren, and Liping Liu in China Meteorological Administration (CMA). Dr. Yanjiao Xiao, Dr. Gaili Wang, Dr. Yabin Gou, and Rongfang Yang also make some help for this research. Thanks to the reviewers and Dr. Yinzhao Ma for their contribution in improving the content and English grammar of this paper. This research was jointly sponsored by the National Natural Science Fund of China (91437214) and the National Key Basic Research Project of China (2012BAC22B04).

References

Adler, R.F., Huffman, G.J., Chang, A., et al., 2003. The version-2 global precipitation climatology project (CPC) monthly precipitation analysis (1979–present). J. Hydrol. 4, 1147–1167.

Anagnostou, E.N., Morales, C.A., Dinku, T., 2001. The use of TRMM precipitation radar observations in determining ground radar calibration biases. J. Atmos. Ocean. Technol. 18, 616–628.

Bolen, S.M., Chandrasekar, V., 2000. Quantitative cross validation of space-based and ground-based radar observations. J. Appl. Meteorol. 39, 2071–2079.

Bringi, V.N., et al., 2011. Rainfall estimation with an operational polarimetric C-band radar in the UK: comparison with a gauge network and error analysis. J. Hydrometeorol. 12, 935–954.

Ciach, G., 2003. Local random errors in tipping-bucket rain gauge measurements. J. Atmos. Ocean. Technol. 20, 752–759.

Cong, F., Liu, L., 2011. A comprehensive analysis of data from the CINRAD and the ground rainfall station. Meteorol. Mon. 37 (5), 532–539.

Gires, A., et al., 2014. Influence of small scale rainfall variability on standard comparison tools between radar and rain gauge data. Atmos. Res. 138 (0), 125–138.

Habib, E., Krajewski, W., Kruger, A., 2001. Sampling errors of tipping bucket rain gauge measurements. J. Hydrol. Eng. 6, 159–166.

Harrison, D.L., Driscoll, S.J., Kitchen, M., 2000. Improving precipitation estimates from weather radar using quality control and correction techniques. Meteorol. Appl. 7, 135–144.

Harrison, D., Scovell, R., Kitchen, M., 2009. High-resolution precipitation estimates for hydrological uses. Proc. Inst. Civ. Eng. 162, 125–135.

Heymsfield, G.M., Geerts, B., Tian, L., 2000. TRMM precipitation radar reflectivity profiles as compared with high-resolution airborne and ground-based radar measurements. J. Appl. Meteorol. 39, 2080–2102.

Huang, L., 2006. Analysis and maintenance of automatic weather station precipitation error. Meteorol. Disaster Reduct. Res. 29 (2), 64.

Jaffrain, J., Berne, A., 2012. Influence of the subgrid variability of the raindrop size distribution on radar rainfall estimators. J. Appl. Meteorol. Climatol. 51 (4), 780–785.

Kim, D., Nelson, B., Seo, D.J., 2009. Characteristics of reprocessed hydrometeorological automated data system (HADS) hourly precipitation data. Weather Forecast. 24, 1287–1296.

Kondragunta, C., Shrestha, K., 2006. Automated real-time operational rain gauge quality controls in NWS hydrologic operations. Preprints, 20th AMS Conf. on Hydrology, 29 Jan.–2 Feb. 2006, Atlanta, GA.

Liao, L., Meneghini, R., Iguchi, T., 2001. Comparisons of rain rate and reflectivity factor derived from the TRMM precipitation radar and the WSR-88D over the Melbourne, Florida site. J. Atmos. Ocean. Technol. 18, 1959–1974.

Moreau, E., Testud, J., Le Bouar, E., 2009. Rainfall spatial variability observed by X-band weather radar and its implication for the accuracy of rainfall estimates. Adv. Water Resour. 32 (7), 1011–1019.

National Meteorological Center of China, 2011. The problems in the provincial automatic gauge rainfall data over China in 2010 and 2011. Technical Report, pp. 1–6 (in Chinese).

Nelson, B., Seo, D.J., Kim, D., 2008. Multi-sensor precipitation reanalysis. Preprints, Int. Symp. on Weather Radar and Hydrology. Laboratoire d'etude des Transferts en Hydroligie et Environnement (LTHE), Grenoble, France, pp. 02–004 (150 pp. [Available online at http://www.wrah-2008.com/PDF/O2-004.pdf.]).

Oye, R., Mueller, C.K., Smith, S., 1995. Software for radar translation, visualization, editing, and interpolation. 27th Conference on Radar Meteorology, Vail, Colo. Am. Meteorol. Soc., pp. 359–361.

Qi, Y.C., Zhang, J., Zhang, P.F., 2013. A real-time automated convective and stratiform precipitation segregation algorithm in native radar coordinates. Q. J. R. Meteorol. Soc. 139 (677), 2233–2240.

Ren, Z., Xiong, A., 2007. Operational system development on three-step quality control of observations from AWS. Meteorol. Mon. 33 (1), 20–22.

Ren, Z., Zhao, P., Zhang, Q., Zhang, Z., Cao, L., et al., 2010. Quality control procedures for hourly precipitation data from automatic weather stations in China. Meteorol. Mon. 36 (7), 123–132.

Rico-Ramirez, M.A., 2012. Adaptive attenuation correction techniques for C-band polarimetric weather radars. IEEE Trans. Geosci. Remote Sens. 50 (12), 5061–5071.

Rico-Ramirez, M.A., Cluckie, I.D., 2008. Classification of ground clutter and anomalous propagation using dual-polarization weather radar. IEEE Trans. Geosci. Remote Sens. 46 (7), 1892–1904.

Rissanen, P., Jacobsson, C., Madsen, H., Moe, M., Palsdottir, T., Vejen, F., 2000. Nordic methods for quality control of climate data. DNMI-Report, No. 10/2000 KLIMA.

Schumacher, C., Houze Jr., R.A., 2000. Comparison of radar data from the TRMM satellite and Kwajalein oceanic validation site. J. Appl. Meteorol. 39, 2151–2164.

Seo, D.J., Breidenbach, J., 2002. Real-time correction of spatially nonuniform bias in radar rainfall data using gauge measurements. J. Hydrometeorol. 3, 93–111.

Shen, Y., Xiong, A.Y., Wang, Y., et al., 2010. Performance of high resolution satellite precipitation products over China. J. Geophys. Res. 115 (Do2114), 17.

Steiner, M., Yuter, S.E., 1995. Climatological characterization of three dimensional storm structure from operational radar and rain gauge data. J. Appl. Meteorol. 34, 1978–2007.

Tollerud, E., Collander, R., Lin, Y., Loughe, A., 2005. On the performance, impact, and liabilities of automated precipitation gauge screening algorithms. Preprints, 21st AMS Conf. on Weather Analysis and Forecasting.

Upton, G., Rahimi, A., 2003. On-line detection of errors in tipping-bucket rain gauges. J. Hydrol. 278, 197–212.

Vasiloff, S.V., Seo, D., Howard, K.W., Zhang, J., Kitzmiller, D.H., et al., 2007. Improving QPE and very short time QPF. Bull. Am. Meteorol. Soc. 60, 1048–1058.

Vejen, F., Jacobsson, C., Fredriksson, U., Rissanen, P., 2002. Quality control of meteorological observations automatic methods used in the Nordic countries. Clim. Rep. 8.

Wang, G.L., Liu, L.P., Ding, Y.Y., 2012. Improvement of radar quantitative precipitation estimation based on real-time adjustments to Z–R relationships and inverse distance weighting correction schemes. Adv. Atmos. Sci. 29 (3), 575–584.

Wang, H.Y., Wang, G.L., Liu, L.P., Jiang, Y., Wang, D., Li, F., 2015. Development of a real-time quality control method for automatic rain gauge data using radar quantitative precipitation estimation. Chin. J. Atmos. Sci. 39 (1), 59–67 (in Chinese).
Wang, J.X., Wolff, D.B., 2009. Comparisons of reflectivities from the TRMM precipitation radar and ground-based radars. J. Atmos. Ocean. Technol. 26, 857–875.
Wang, S.D., Pei, C., Guo, Z.M., Shao, N., 2011. Evaluation on Chinese next generation radars coverage and terrain blockage based on SRTM data. Clim. Environ. Res. 16 (4), 459–468.
Wen, Y.X., Hong, Y., Zhang, G.F., Schuur, T.J., Gourley, J.J., Flamig, Z., Morris, K.R., Cao, Q., 2011. Cross validation of spaceborne radar and ground polarimetric radar aided by polarimetric echo classification of hydrometeor types. J. Appl. Meteorol. Climatol. 50, 1389–1402.
Xiao, Y., Liu, L., 2006. Study of methods for interpolating data from weather radar network to 3-D grid and mosaics. Acta Meteorol. Sin. 64 (5), 647–657.
Xie, P.P., Arkin, P.A., 1996. Analyses of global monthly precipitation using gauge observations, satellite estimates, and numerical model predictions. J. Clim. 9, 840–858.
Zhang, J., Langston, C., Howard, K., 2008. Brightband identification based on vertical profiles of reflectivity from WSR 88D. J. Atmos. Ocean. Technol. 25, 1859–1872.
Zhang, P., Du, B., Dai, T., 2001. Radar Meteorology. Meteorological Press, China (177–216 pp.).
Zhang, Y., Adams, T., Bonta, J.V., 2007. Subpixel-scale rainfall variability and the effects on separation of radar and gauge rainfall errors. J. Hydrometeorol. 8 (6), 1348–1363.
Zhong, L., Liu, L., Gu, S., 2007. An algorithm of identifying convective and echo in mixed precipitation and its application in estimating rainfall intensity. Plateau Meteorol. 26 (03), 593–602.